ISSN 1392–1207. MECHANIKA. 2020 Volume 26(5): 407–415

Numerical Study on Thoracic Aortic Aneurysms: The Aneurysm Aggravation Effects on the Secondary Flow Motion

Mohammed Ilies ARAB*, Mohamed BOUZIT*, Houari AMEUR, Youcef KAMLA*****
**Faculty of Mechanical Engineering, USTO-MB, 1505 El M'naouar, Oran, Algeria,*
E-mail: m.arab@univ-usto.dz (Corresponding Author)
***Department of Technology, Ahmed Salhi University Centre of Naama, PO Box 66, Naama 45000, Algeria*
****Faculty of Sciences and Technology, Hassiba Ben Bouali University of Chlef, Algeria,*
E-mail: kamla_youcef@yahoo.fr

crossref http://dx.doi.org/10.5755/j01.mech.26.5.23254

1. Introduction

The Computational fluid dynamics (CFD) approach on hemodynamic problems provided numerous insights in the understanding of cardio-vascular diseases (CVDs), their genesis and impact on blood flow. The complexity of the thoracic aorta (TA) geometry combined with oscillating character of the flow give rise to complex phenomena such as Dean and Lyne vortices [1]. The secondary flow importance in avoiding CVDs and therefore ensuring the good functioning of the cardio-vascular system is proved, especially in avoiding blood components stagnation in curved arteries that could lead to arterial disease such as atherosclerosis [2]. Similarly, Liu et al. [3] studied the effects of the Pulsatile character and the blood flow secondary motion (vortices) on mass transport of different components such as Low-density lipoprotein (LDL) and oxygen (O_2) distribution which can lead to arterial tissue damages. Dean & al. [4] first developed under the assumption of a uniform axial velocity distribution an analytical solution for steady flows in bends characterized by relatively low Dean numbers. Unsteady periodic flows in bends are characterized by the Dean (De) and Womersley (Wo) numbers. Sudo et al. [5] studied experimentally unsteady periodic flows and gave a classification of five types of vortices mapped in function of Dean and Womersley numbers. Boiron et al. [6] studied experimentally and numerically the different parameters and mechanisms involved in the apparition of secondary flows in a bend under physiological conditions. Glenn et al. [7] deduced experimentally a regime map for the number of vortices function of dimensionless parameters for physiological and non-physiological periodic non zero-mean flows; this last also underlined the importance of the boundary layer in the formation of the secondary motion.

Manifold studies on the influence of the flow characteristics on the formation of CVDs that implies arterial deformation can be found in the literature [8]. Tan Despite the numerous studies on TAAs, the impact of this last on the secondary flow and its underlying phenomena remain unclear. Several authors studied the resulting flow phenomena such as the vortex ring especially for the Abdominal aortic aneurysm (AAA). Finol et al. [9] and Ge et al. [10] described the vortex ring (VR) dynamics in three steps (i) the formation of the ring (ii) the vortex ring stall (iii) finally the rupture and dissipation of the ring with an impingement towards the distal part of the aneurysm. However, the phenomenon remains unstudied in the case of (TAA) and the conjugated effects of the curvature and the enlargement can lead to variations on the flow structure and the underlying phenomena.

The Newtonian blood rheology assumption is generally accepted for large and healthy arteries, however arterial diseases such as atherosclerosis or aneurysms creates hydrodynamic instabilities and therefore causes oscillating shear stresses, in this case the Newtonian model is not valid anymore. Palacios-Morales [11] studied experimentally the effects of the shear-thinning model on the (VR) dynamics. They found that the propagation of the ring is proportional to the power index "*n*". Then, Deplano et al [12] studied experimentally the effects of shear thinning character of blood on the vortex ring behavior inside (AAA) in terms of shear stress and velocity propagation. Nevertheless, to this date, no study has been done on the phenomenon for the (TAA) and this is mainly due to its rarity compared to (AAA). However, the occurrence of this disease is increasing [13] and this study aims to reduce this lack of information.

As a phenomenon, the vortex ring and their interaction with walls is widely studied in literature. Liu [14] studied the interactions with both inclined and perpendicular walls and enlightened the creation of a recirculation motion at the impingement of the ring on the wall. The phenomenon inside aneurysms implies the confinement of the ring. Stewart et al. [15] studied the effects of this parameter on the ring dynamics and showed that the confinement has an influence on the rate of decay of the ring.

The primary flow is also a subject of matter concerning the evolution of the aneurysm. The clinical research studies of Den Reijer et al [16] showed a correlation between entrance angle of the jet and the dilatation of aneurysms. Arzani and Shadden [17] showed that in some cases the primary jet stays coherent inside the aneurismal bulge and in these cases the vortex ring recirculation is stronger. The strength of the vortex ring can lead to a deflection of the primary jet towards the artery wall which can lead to further weakening of this last, therefore the present study also focuses the variations of the primary jet and its impact area with respect to the aggravation of the aneurysm.

2. Presentation of the problem

Thoracic aortic aneurysms (TAA) is defined as a localized diameter enlargement situated in the ascending part of the aorta, this last one is a silent disease generally

with a slow evolution 0.1 cm/year [13]. We used the geometry presented in the experimental work of Boiron et al. [6] as a starting point to validate our numerical model. This last is a U-shaped Tube Fig. 1 a, with a constant circular cross sectional diameter of 2.2 cm, the inlet and the outlet tube lengths are 10 and 20 times the radius respectively. The curvature is the most important feature of the geometry and the flow in general, it is characterized by the ratio r/R (delta = 0.073) and consequently the Dean number, this one was specially chosen to match with physiological characteristics, the dimensions are recapitulated in Table 1.

To investigate the effects of the enlargement on the downstream flow and the vortex formation conditions, we have added a pseudo-idealistic and asymmetric enlargement centered at θ = 30° form the entrance with a maximal enlargement of two and three times the normal diameter respectively represented in (Figs. 1 b – c). More details about the aneurysm dimensions are summarized in Table 2.

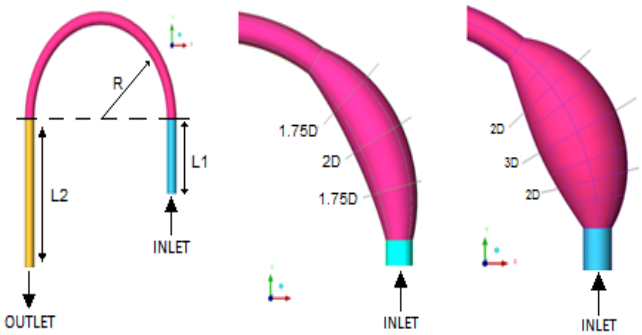

a) Case 1 b) Case 2 c) Case 3

Fig. 1 Studied geometries

Table 1

Geometry dimensions

Parameter	r, cm	L_1, cm	L_2, cm	*Delta*
Value	1.1	10*r	20*r	0.073

Table 2

Dimensions of the aneurysms

Angles	Diameters, cm	
	Case 2	Case 3
15°	3.85	4.4
30°	4.4	6.6
45°	3.85	4.4

3. Materials and methods

The blood Rheology is a common topic in the literature but remains unclear, the rheological behavior varies with respect to the hematocrit fraction and the diameter of the studied artery. Since the blood plasma is well known to be Newtonian, there is no doubt that the rheological complexity is due to the nature of the suspensions (hematocrit) and their effects are inversely proportional to the vessel diameter. The rheological behavior is mostly described by two kinds of models. First, models that predicts the shear-thinning effects such as the Carreau model, which gives a good agreement with the experiment but tends to overestimate the shear stress limit at which the blood behavior becomes Newtonian. Secondly the blood behavior is described by yield stress models such as the Casson model which gives a good approximation for low strain rate values but overestimate the wall shear stress (WSS) for high strain rates. The generalized power law is a good approach for studies that implies the non-Newtonian behavior [18, 19]. This last one is in good agreement with the Carreau model for low strain rates and gives a good approximation for higher values of strain. For the present study, the Newtonian assumption is used to validate the numerical model; this assumption is justified for the normal case (case 1) by numerous studies in the literature [3, 7].

Fung [20] stated that the shear stress range in the aorta is way above the critical value of 100 s^{-1}. According to Caballero et al. [21], the blood is Newtonian for shear stress values above this level. However, for the diseased cases the shear-stresses inside the aneurysm bulge are highly oscillating and therefore the Newtonian hypothesis is no more valid. To correctly investigate the vortex ring behavior inside the aneurysm we used the power law to mimic the shear-thinning effects inside the aneurysm with a consistency K = 0.0034 $Pa.s^{n-1}$ and a structural index n = 0.6. This model is known to give good approximation for the complex blood rheology [22].

3.1. Numerical model

We used for the present study the ANSYS CFX 13 software to validate our numerical model against the experiment. We used the SST turbulence model which is often used in literature for such problems [23]. We performed a successive re-meshing until the acceptable precision in Fig. 2. The final mesh strategy was a hexahedral mesh of 1.6 million elements the maximal mesh size on the length is 10^{-3} and 53 elements over the diameter (Fig. 3).

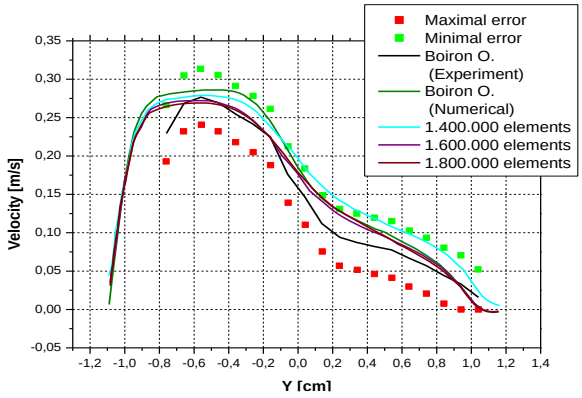

Fig. 2 Mesh performance tests

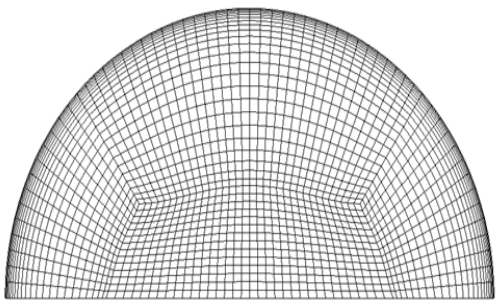

Fig. 3 Face mesh of the cross sectional area

The same time step of the study presented by Boiron et al. [6] (Δt = 0.002 s) was taken, and the convergence criterion on residuals was set to 10^{-6}. The solved mathematical model is the following:

Continuity equation:

$$\frac{\partial \rho}{\partial t} + \vec{\nabla}.(\rho \vec{V}) = 0;$$

Conservation of momentum:

$$\frac{\partial \rho}{\partial t} + \vec{\nabla}.(\vec{V} \otimes \vec{V}) = -\vec{\nabla}P + \mu\left[\nabla^2 \vec{V} + \frac{1}{3}\vec{\nabla}(\vec{\nabla}.\vec{V})\right].$$

For the Non-Newtonian part of the study, the following power law model was used:

$$\mu = \mu_0 \dot{\gamma}^{(n-1)},$$

where: the consistency μ_0 = 0.0034 Pa.s^{n-1} and the structural index n = 0.6.

3.2. Boundary conditions

At the inlet: the main issue of the study is to understand the implications of the unsteady nature of the flow on the vortex creation, in a bended duct with a localized deformation at the arch entrance. To do so, we used a physiological velocity inlet function over one cardiac cycle represented (Fig. 4) characterized by a Dean number that relates the centripetal and inertial forces to the viscus force (De = 301), and a Womersley number that expresses the transient inertial forces with relation to the viscous forces (Wo = 12.85), where: $De = Re\sqrt{\frac{r}{R}}$ and $Wo = r\sqrt{\frac{\omega\rho}{\mu}}$,

where: Re is Reynolds number; r is artery radius; R is the radius of curvature; ω is the angular frequency of the flow oscillation and ρ the density.

At the artery wall: in order to avoid the memory cost of unsteady numerical simulations we have chosen to use the rigid wall assumption. At the outlet: we used the zero pressure boundary condition at the outlet.

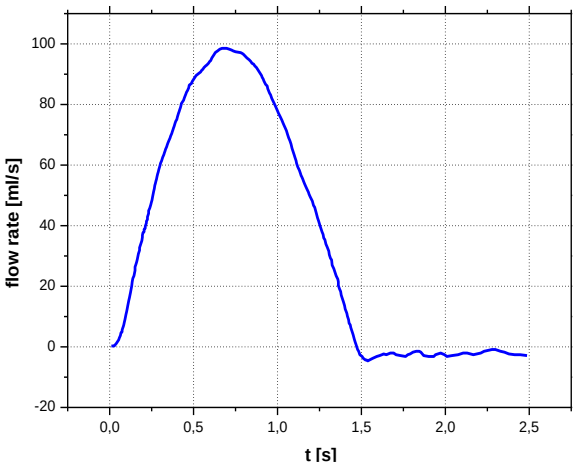

Fig. 4 Inlet velocity signal

4. Results

The numerical results were validated against the experimental study of Boiron et al. [6] and the numerical study of Keshavarz-Motamed et al. [24]. As we can see in Fig. 5, our numerical results are in good agreement with both cited studies.

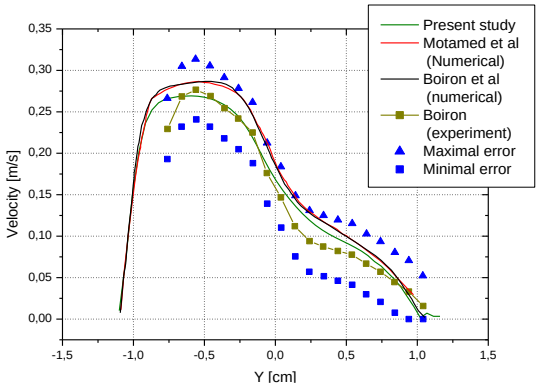

Fig. 5 Axial velocity profile at 90°, t = 1.05 s

4.1. Influence of the aneurysm on the secondary motion

For both aneurysm cases (case 2 & 3) results are nearly the same, thus we have chosen to compare only the case 1 & 2 in Figs. 6 and 7 respectively where velocity streamlines for different cross section angles over whole cycle are represented.

As expected, the vortex creation in a curved artery for an unsteady periodic flow exhibits a complex behavior. It can be seen that the process is triggered at the mid systole phase t = 0.36 s characterized by a low velocity inlet, where we can already distinguish two symmetric counter-rotating vortices near the outer wall from the entry of the first quarter of the aortic arch to its end Figs. 6 a – d. At the end of the systole (t = 0.66 s) the inlet velocity rises, the two precedent vortices tend to be pushed towards the inner side of the bend. This configuration is the preliminary step of the formation of type II dean vortices Figs. 6 e – h which can be noticed for flows with a Wo slightly superior to 10, at this point no difference between case 1 & 2 can be seen. At the beginning of the diastole phase (t = 1.05 s) we can see for the case 1 that the velocity peak shifts towards the outer side of the bend Fig. 5. While this shift is less pronounced for the case 2. As a result, a stagnant region is formed near the outer side of the curvature for the case 1 only, and then we can see the apparition of bean shaped vortices called type II (Figs. 6, i - l), form an angle of 45° to the outlet of the arch.

For the case 2 this configuration is delayed to the third quarter of the arch (approximately 135°) Figs. 7, k - l. At the end of the diastole (t = 1.35 s) we can see the formation of deformed type II dean vortices at 45° from the entrance of the bend to its end, as described by Sudo et al [5] for flows with Wo in the range of 11 to 13 as imposed by the physiological conditions in the aorta. We also noticed the formation of two additional counter-rotating vortices (also rotating in the inverse sense of the two precedent ones) at the center of the artery from 90° to nearly 180° (Figs. 6, r - t). For the case 2 this last configuration never occurs in the middle of the arch (90°) Fig. 7 r and is retarded until the 135°, these two new vortices are also weaker (Fig. 7, s) and they tend to disappear in the last quarter of the arch (Fig. 7, t).

4.2. Effects of the Aneurysm aggravation and blood rheology on the vortex ring dynamics

In order to study the progression of the vortex ring inside the aneurysm we have drawn four progression lines

starting from 5 degrees of the aneurysm entry and disposed 15 degrees from each other for both aneurysm cases Fig. 8.

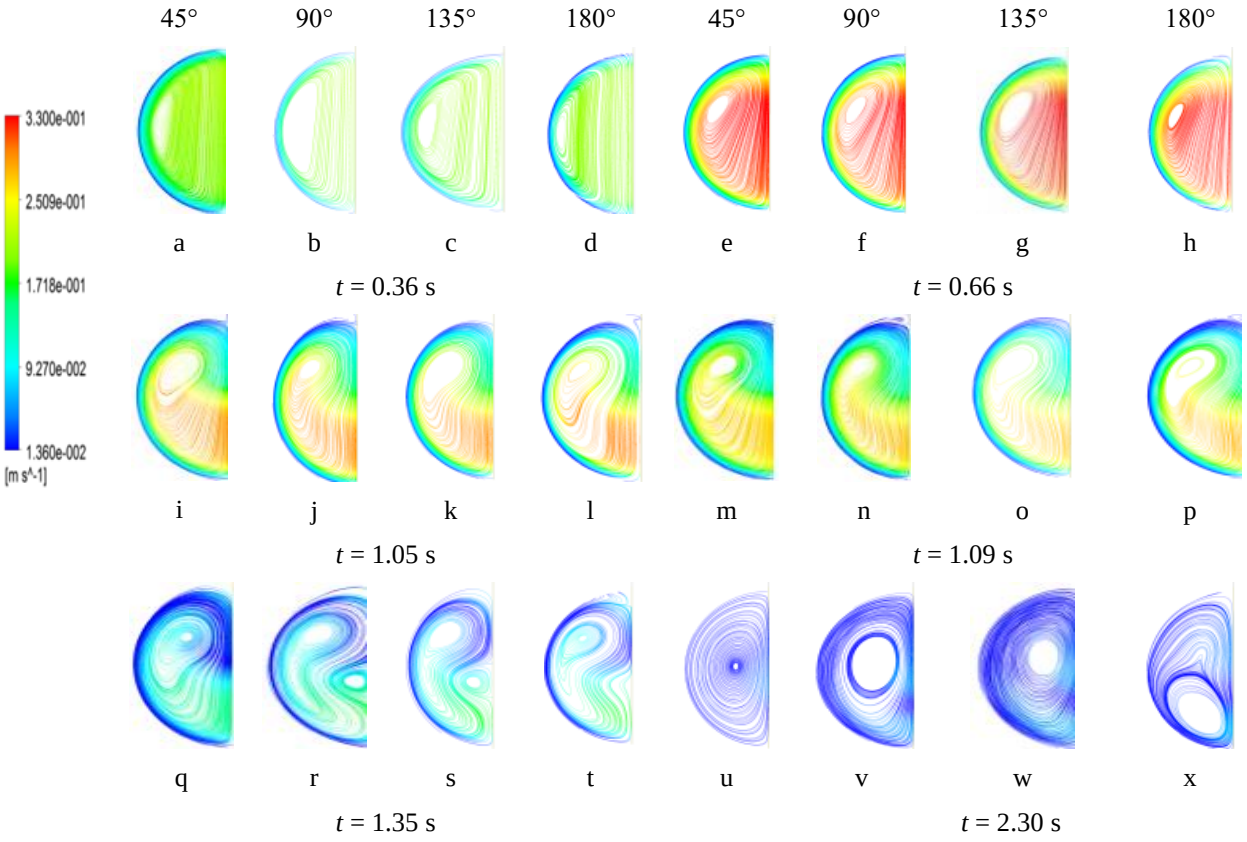

Fig. 6 Velocity streamlines at different cross section angles for case 1 over the cycle

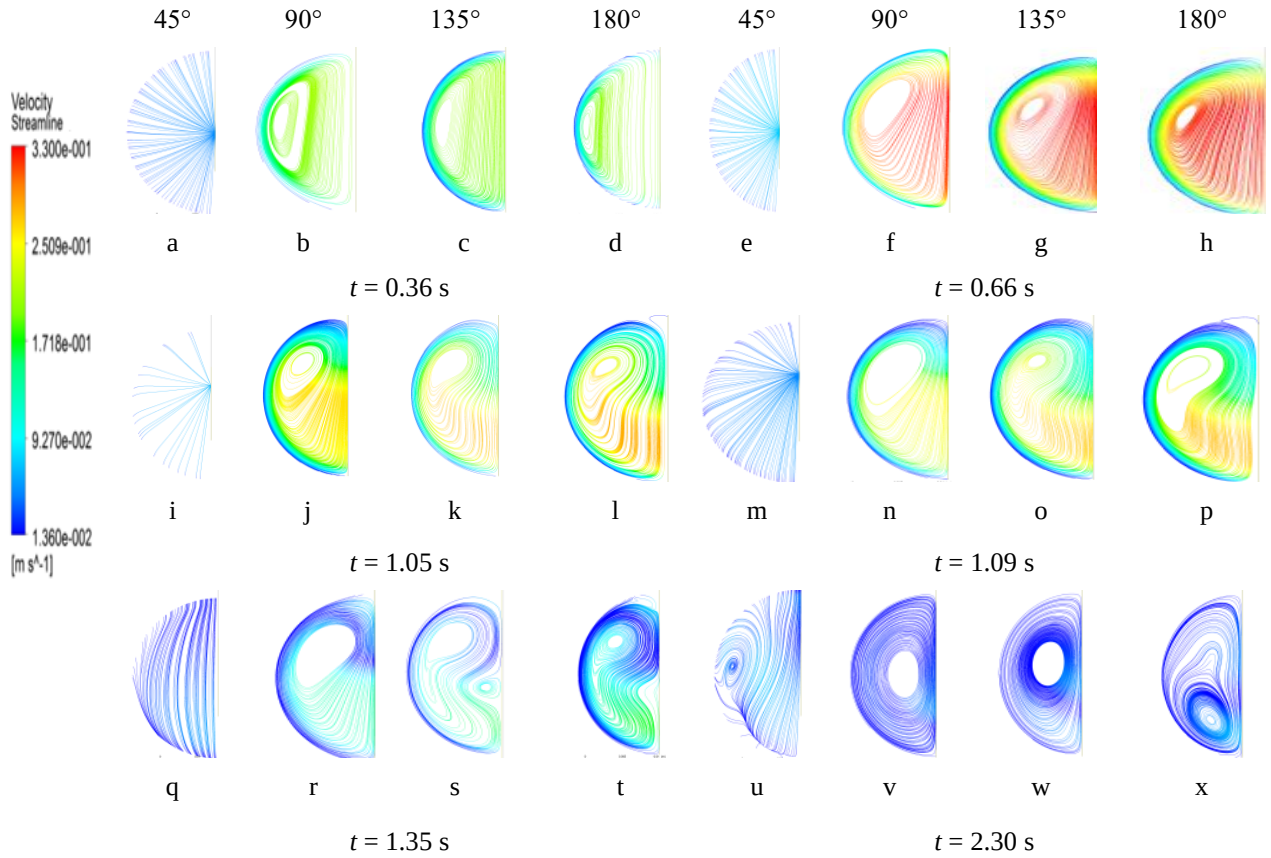

Fig. 7 Velocity streamlines for different cross section angles over the cycle for aneurysm, case 2

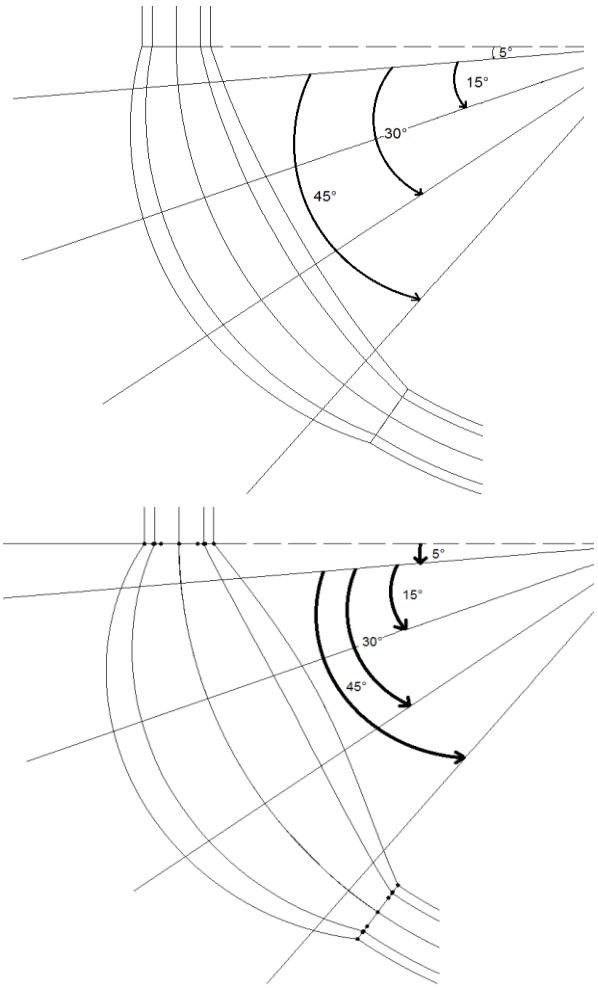

Fig. 8 Progression lines disposition

4.2.1. Effects of the aggravation on the vortex ring dynamics

The vortex ring dynamics inside the aneurysm can be described in three steps: the formation of the vortex ring, the evolution of the ring inside the aneurysm (the stall and expansion phase) and finally the vortex impingement and decay.

1. We can see that the vortex ring is formed and strengthens during the systole phase. At the early stage of the cycle we can already remark differences between case 2 & 3 where the vortex rings appear at different moments t = 0.5 s and t = 0.36 s respectively, represented in 2D by two counter rotating vortices situated after the entry of the aneurysm neck on both inner (IS) and outer sides (OS) of the bend. During the rest of the systole until t = 0.664 s when the inlet velocity is at its maximum, the vortex ring strengthens for both cases but in different manners, we can clearly remark that case 2 vortices are stretched axially (Fig. 9, b 1), while they expend radially for the case 3, these lasts are also larger (Fig. 9, b 3).

2. The diastole phase marks the beginning of the stall and expansion process. At t = 1.09 s, the vortex ring for the case 2 is stalled from the (IS) wall and continues its radial expansion, while the (OS) vortex is confined at the aneurysm wall by the primary flow Fig 9, c 1. This unilateral motion indicates a rotation of the ring in the clockwise direction. On the other hand, for the case 3 both sides of the vortex ring are stalled from the entrance neck, so the rotation of the ring is less important than the case 2. At this step of the process, they move along the centerline and expend radially. The (OS) vortex is also stretched axially and the displacement of this last creates a small recirculation region behind (OS) vortex in Fig. 10.

3. The process ends with the impingement then the decay of the vortex ring and we can clearly note that this phase starts earlier for the case 2. As the vortex ring rotates and thus as the (IS) vortex approaches the (OS) wall, we remark the generation of an inverse secondary motion on this last and next to the vortex ring at t = 1.2 s (Fig. 11), this marks the beginning of the impingement of the (IS) vortex on the (OS) wall. At t = 1.35 *s*, the (OS) vortex weakens and the IS and the inverse secondary motion strengthens. For the case 3 at t = 1.37 s the (OS) vortex is still active but weakens. While the (IS) vortex finally impacts the (OS) wall; an inverse secondary motion appears because of the ((IS) vortex/(OS) wall) interaction. At the end of the cycle, even if the ring decays in the same manner for both aneurysms by the weakening of the (OS) vortex, we remark that the ring breaks at different moments for the two cases (case 2: t = 1.6 s; case 3: t = 2.1 s). At t = 2.3 s we can note for the case 2 that after the break of the ring, the (OS) vortex decays and its diameter diminishes, this makes it easier for the next inlet pulse to wash away the deposits. On the contrary for the case 3, the remaining vortex cell of the ring ((IS) vortex) stays active and large enough to ensure recirculation in the entire aneurysm cavity, this could make the clearing of the aneurysm bulge more difficult, augment the residence time and therefore enhance the probability of thrombosis.

4.2.2. Effects of the blood rheology on the vortex ring dynamics

The analysis of the vortex ring motion across the progression lines during the successive time steps permitted to highlight some differences in the ring dynamics between the shear thinning and the Newtonian models. First, the ring motion for both aneurysm cases is slower when the shear-thinning model is used. Differences can be seen during the diastolic phase, at t = 1.09 s for the case 2 we remark for the Newtonian model that the (IS) vortex passes the second line while this last is still in between the first two lines. This delay is conserved during the rest of the cycle Figs. 9, c1 – c2, the same phenomenon can be noticed while comparing the Newtonian and shear thinning predictions for the case 3. Table 3 shows the different impingement angles from the entry of the aneurysm.

Table 3

Impingement angles

	Newtonian	Shear-thinning
case 2	25°	18°
case 3	35°	30°

4.3. The primary jet and vortex ring interaction

We note through the analysis of the phenomenon development that the (primary jet/vortex ring) interaction can be described in two phases. First, during the systolic phase when the primary jet is in constant acceleration and the ring is created by the recirculation motion at the aneurysm entrance neck. The size and the vorticity increase as the inlet velocity increases, in this phase the primary jet is

too strong to be influenced by the ring. The second step of the phenomenon happens during the diastolic phase where the velocity inlet decreases and therefore the primary jet weakens at the same time the vortex ring is stalled from the aneurysm neck and expands. The expansion of the (IS) vortex deflects primary jet, in this phase the primary jet angle depends on the orientation of the ring core Fig. 9, b 1, c 1, b 3, c 3. The aneurysm morphology has an influence on the vortex ring dynamics and thus have an influence on the primary jet deflection. We can note from the comparison of case 2 & 3 aneurysm that the jet is deflected towards the proximal part of the (OS) wall for Case 2 (Fig. 9, d 1), while the deflection is done towards the distal part of the (OS) wall (Fig. 9, d 3).

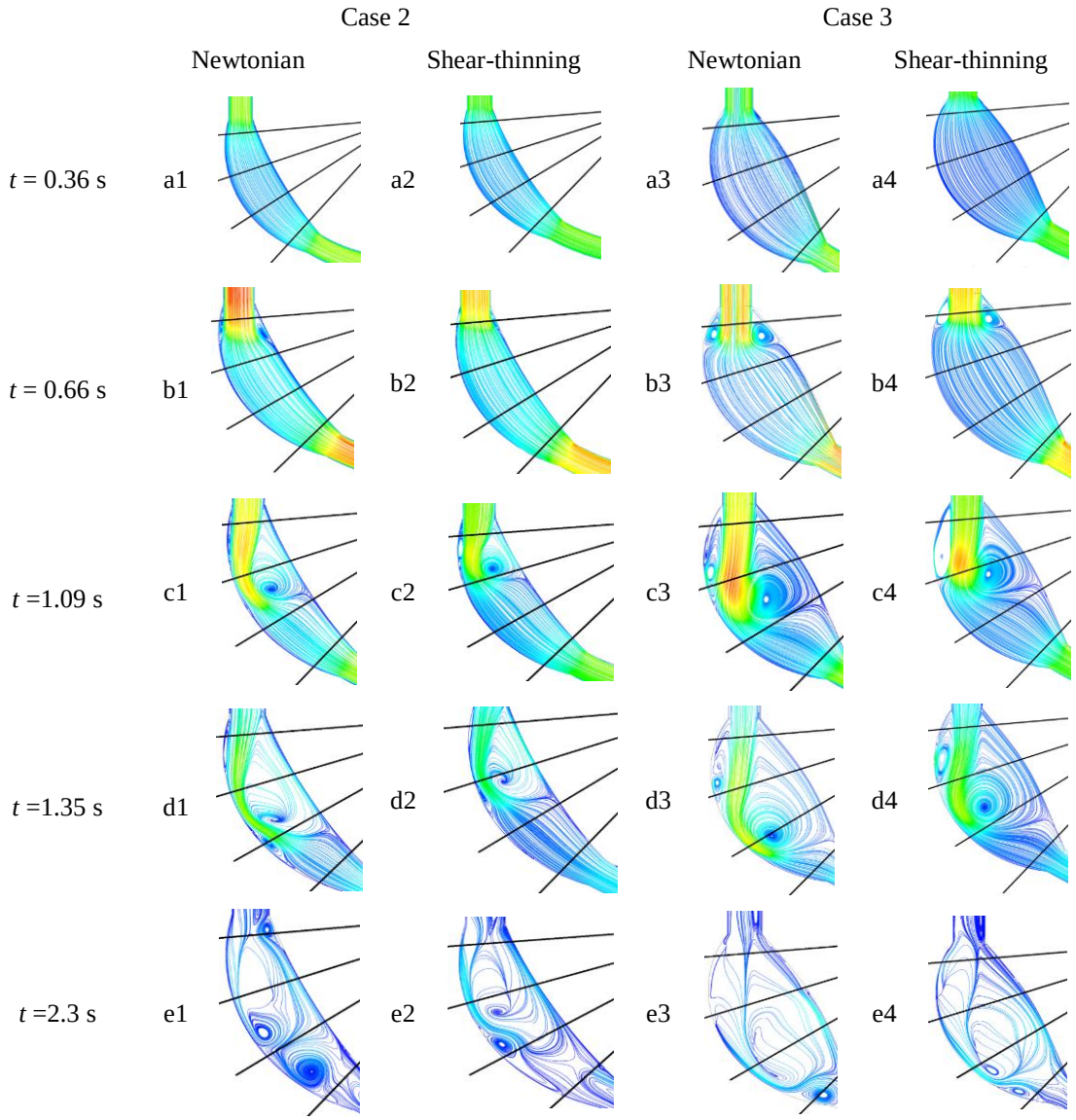

Fig. 9 Velocity streamlines for both aneurysm cases with the Newtonian and shear-thinning models

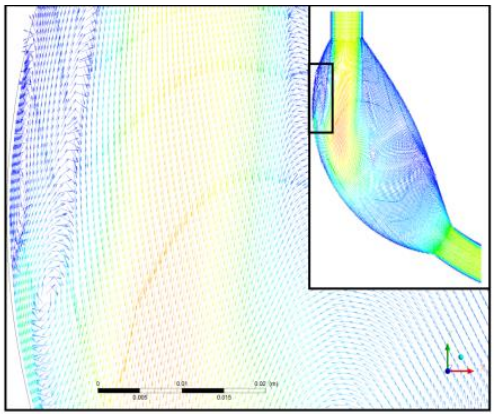

Fig. 10 Inverse secondary recirculation secondary motion behind the OS vortex at t = 1.09 s for Case 3

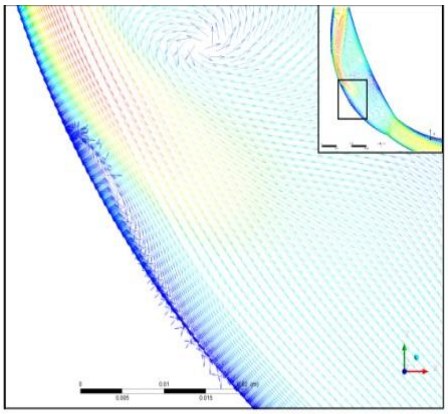

Fig. 11 Apparition of the inverse motion next to the OS impingement area at t = 1.2 s for Case 3

5. Discussion

5.1. Effects of the aneurysm on the secondary motion

The formation of two weak counter-rotating vortices in the beginning of the process (t = 0.36 s), near the lateral walls and centered in the median of the cross section plan is due to the balance between the centrifugal forces and the conjugate action of the pressure gradient and viscous forces. Later in the process at the end of the systole phase (t = 0.66 s) inertial forces are stronger and concentrated at the center of the artery. This makes the pressure gradient push the precedent vortices towards the inner side of the artery bend. No differences can be seen between the diseased geometries and the normal case, this can be explained by weakness of the hydrodynamic instabilities inside the aneurysm in comparison to the primary flow, these lasts are insufficient to disturb the stokes boundary layer. Later on, at the beginning of the diastole phase (t = 1.05 s) we can see in the case 1 that velocity peak shifts towards the outer side of the bend (Fig. 5), which is an important indicator for dean instabilities occurrence, the shift in question is not as pronounced for the diseased cases (Fig. 12).

From this step, the process involves in different ways for the normal and the diseased cases. The helical flow formation is altered and retarded downstream the aneurysm, at t = 1.35 s. Lyne vortices never occur in the aortic arch center for the aneurysm cases, which is the most vulnerable part to blood stagnation. This fact can be explained by the induced hydrodynamic instabilities inside the aneurysm that disturbs the stocks boundary layer. Glenn et al. [7] have noticed similar effects with a stent-induced perturbation that reduces the secondary motion in aorta.

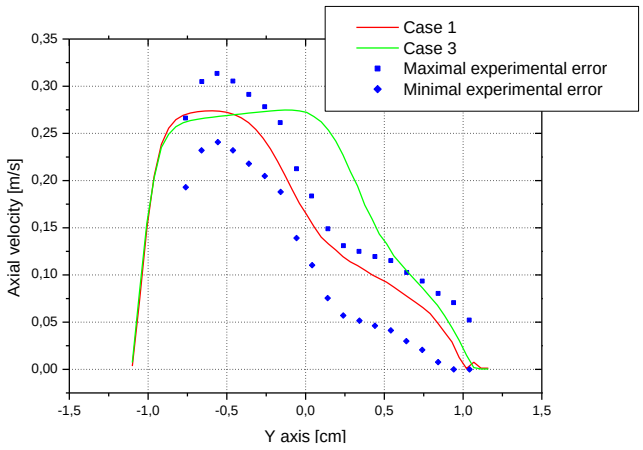

Fig. 12 Velocity shift comparison at position 90° and t = 1.05 s

5.2. Effects of the Aneurysm aggravation on the Vortex ring (VR) dynamics

Due to the lack of studies concerning the vortex ring phenomenon in the (TA) aneurysm our results were compared to studies concerning Abdominal Aortic Aneurysms (AAA). The three phases described earlier are in agreement with the literature Ge et al. [10]. The process of creation and development of the vortex ring was also observed by Deplano et al. [12], where the ring is created during the systolic acceleration this last is stalled from the entry neck at the mid-diastole then propagates in the aneurysm bulge, finally the impingement & decay of the ring happens during the rest of the cycle.

The creation of the vortex ring phase is a conditioning step, the delay in the vortex creation for the case 2 aneurysm compared to the case 3 explains the differences in the process development during the rest of the cycle. This delay is due to the severity of the aneurysm; the aspect ratio of the aneurysm is a key factor for the development of vortex rings in aneurysms. Unlike the (AAA) especially for symmetric geometries where both sides of the ring affect the distal part of the aneurysm nearly at the same time. Only the (IS) vortex impinges on the (OS) wall of the aneurysm for the (TAA). The breaking of the ring is done by the disappearance of the (OS) vortex. Finally, the decay of the vortex ring in the case 2 happens earlier in the cycle compared to the case 3, this can be explained by the confinement which is known to augment the rate of decay.

5.3. Effects of the Non-Newtonian characteristic on the (VR) dynamics

The propagation velocity of the vortex ring is less important for the shear-thinning model, the vorticity is weaker and therefore vortices are also smaller this explains why no inverse secondary motion can be seen at the back of the vortex ring after the stall of the IS for the case 3 Figs. 9, c4, d4. This phenomenon can be explained by the fact that the vortex ring strength and vorticity are created and conditioned by primary jet and its velocity peak, as we can see Fig. 9, b1 to b4 and Fig. 9, c1 to c4 this last is less important for shear-thinning fluids because of the viscous effects on the boundary layer [11].

5.4. Influence of the hydrodynamic instabilities and the rheological model on the primary jet

It is well known that the hydrodynamic parameters have a significant impact on arterial diseases especially on aorta's aneurysms and their evolution. In case of diseases resulting in a geometrical variation, a two-way relationship between the evolution of the sickness and the flow dynamics is established. The usual argumentation found in the literature is often correlated to the variations in (WSS) distribution [24]. However, other authors [15] relate it to the primary flow jet for patients presenting a Bicuspid arterial valve (BAV) studies on the effects of the jet intensity and its direction on the aggravation of $(TAA)_s$ and our work dovetail in a similar optic as Arzani et al. [17]. The Newtonian model predicts a greater area of the jet impingement on the (OS) wall (Fig. 9, d1 & d3) then the shear-thinning model (Fig 9, d2 & d4.) This can lead to an under estimation of the rupture risks as these lasts are correlated with small impingement areas. Since the vortex ring does not propagate for the shear-thinning as far as the Newtonian model, the impingement zone also varies (Table 3) and thus the predicted rupture area can also be biased by the rheological model choice.

6. Conclusion

This study aims to investigate effects of a variation in the morphology of the aorta during the aggravation of the aneurysmon the vortex ring phenomenon at first and the changes on secondary flow motion and the related phe-

nomena (Dean and Lyne vortices) downstream the enlargement. These lasts are present in all over the artery network and their importance in the efficiency and the good health of the artery walls is proved, which makes the following conclusions easily extrapolated to the other curved arteries.

- The aneurysm clearly reduces the intensity of the dean vortices in the diastolic phase downstream, Lyne vortices creation is delayed to the position 135° also with less intensity. This shows that the immediate region after an aneurysm is prey to diseases due to stagnation of different blood substances such LDL or a lack of oxygenation that could alter the downstream artery walls.

- The vortex ring is clearly affected by the rheological model in terms of the ring propagation, vorticity and jet intensity, thus the Newtonian model can lead to misconceptions in the phenomena occurring inside the aneurysm. The VR propagation velocity is lower for the shear-thinning model compared to the Newtonian model which is in agreement with experimental studies; the power law model is therefore more suitable when studying vortex ring dynamics.

- The size of the aortic bulge plays an important role in the break of vortex rings, the early break of the ring for small aneurysms reduce the residence time and therefore reduce the occurrence chances of thrombosis.

- The redirection of the primary jet by the VR is to the author's opinion a key factor in the mechanism by which the augmentation of stress occurs on the artery wall, and therefore is the principal cause in the vicious circle of the deformation increase and hydrodynamic instabilities (vortex ring) inside the aneurysm. The use of the shear-thinning model is also suitable when studying the stress on the artery walls since the rheological model influences the vortex ring impingement area and thus the primary jet impact.

References

1. **Lyne, W. H.** 1970. Unsteady viscous flow in a curved pipe, J. Fluid Mech. 45(1): 13-3.
2. **Hong, J.; Wei, L.; Fu, C.; Tan, W.** 2008. Blood flow and macromolecular transport in complex blood vessels, Clinical Biomechanics 23: S125–S129. https://doi.org/10.1016/j.clinbiomech.2007.07.006.
3. **Liu, X.; Fan, Y.; Deng, X.; Zhan, F.** 2011. Effect of non-Newtonian and pulsatile blood flow on mass transport in the human aorta., Journal of Biomechanics 44: 1123–1131. https://doi.org/10.1016/j.jbiomech.2011.01.024.
4. **Dean, W. R.; Hurst, J. M**. 1927. Note on the motion of fluid in a curved pipe, The London, Edinburgh, and Dublin Philosophical Magazine and Journal of Science, series 7, 4(20): 208–223. https://doi.org/10.1080/14786440708564324.
5. **Sudo, K.; Sumida, M.; Yamane, R;** 1992. Secondary motion of fully developed oscillatory flow in a curved pipe., J. Fluid Meeh. 237: 189-208.
6. **Boiron, O.; Deplano, V.; Pelissier, R.** 2007. Experimental and numerical studies on the starting effect on the secondary flow in a bend, J. Fluid Mech. 574: 109–129. https://doi.org/10.1017/S0022112006004149.
7. **Glenn, A. L.; Bulusu, K. V.; Shu, F.; Plesniak M. W.** 2012. Secondary flow structures under stent-induced perturbations for cardiovascular flow in a curved artery model., International Journal of Heat and Fluid Flow 35: 76–83. https://doi.org/10.1016/j.ijheatfluidflow.2012.02.005.
8. **Tse, K. M.; Chiu, P.; Lee, H. P.; Ho, P.** 2011. Investigation of hemodynamics in the development of dissecting aneurysm within patient-specific dissecting aneurismal aortas using computational fluid dynamics (CFD) simulations., Journal of Biomechanics 44: 827–836. https://doi.org/10.1016/j.jbiomech.2010.12.014.
9. **Finol, E. A.; Keyhani, K.; Amon, C. H**. 2013. The Effect of Asymmetry in Abdominal Aortic Aneurysms Under Physiologically Realistic Pulsatile Flow Conditions, Journal of Biomechanical Engineering, vol. 125. https://doi.org/10.1115/1.1543991.
10. **Ge, L.; Kassab, G. S.** 2010. Turbulence in the Cardiovascular System: Aortic Aneurysm as an Illustrative Example., Computational Cardiovascular Mechanics. https://doi.org/10.1007/978-1-4419-0730-1_10.
11. **Palacios-Morales, C.; Zenit, R.** 2013.The formation of vortex rings in shear-thinning liquid, Journal of Non-Newtonian Fluid Mechanics 194: 1–13.
12. **Deplano, V. Y.; Knapp, B.; Bailly, L; Bertrand, E.** 2014. Flow of a blood analogue fluid in a compliant abdominal aortic aneurysm model: Experimental modelling, Journal of Biomechanics. http://dx.doi.org/10.1016/j.jbiomech.2014.02.026.
13. **Elefteriades, J. A.; Farkas, E. A.** 2010. Thoracic Aortic Aneurysm, Journal of the American College of Cardiology 55(9).
14. **Liu, C. H.** 2002. Vortex simulation of unsteady shear flow induced by a vortex ring, Computers & Fluids 31(2): 183–207. https://doi.org/10.1016/S0045-7930(01)00018-4.
15. **Stewart, K. C.; Niebel, C. L.; Jung, S.; Vlachos, P. P.** 2012. The decay of confined vortex ring, Exp Fluids 53: 163–171. https://doi.org/10..1007/s00348-012-1277-5.
16. **Den Reijer, M.** 2010. Hemodynamic predictors of aortic dilatation in bicuspid aortic valve by velocity-encoded cardiovascular magnetic resonance. J. Cardiovasc. Magn. Reson. https://doi.org/10.1186/1532-429X-12-4.
17. **Arzani, A.; Shadden, S. C.** 2012. Transport and mixing in patient specific abdominal aortic aneurysms with Lagrangian coherent structure, Proceedings of the ASME, Summer Bioengineering Conference SBC2012, Farjardo, Puerto Rico, USA.
18. **Ameur, H**. 2016. Effect of some parameters on the performance of anchor impellers for stirring shear-thinning fluids in a cylindrical vessel, J. Hydro. 28: 669-675. https://doi.org/10.1016/S1001-6058(16)60671-6.
19. **Ameur, H**. 2018. Pressure drop and vortex size of power law fluids flow in branching channels with sudden expansion, J. Appl. Fluid Mech. 11: 1739-1749. https://doi.org/10.29252/jafm.11.06.28831.
20. **Fung, Y. C.** 1993. Biomechanics mechanical proprieties of living tissues second edition, Springer.
21. **Caballero, A.; D, Lain S.** 2013. A review on computational fluid dynamics., Modelling in Human Thoracic

Aorta, Cardiovascular Engineering and Technology 4: 103–130.
https://doi.org/10.1007/s 13239-013-0146-6.

22. **Soulis, J. V.; Lamprio. P.; Fytanidisd. K., Giannoglou G. D**. 2011. Relative residence time and oscillatory shear index of nonnewtonian flow models in aorta, Biomedical Engineering, 2011 10th International workshop.
https://doi.org/10.1109/IWBE.2011.6079011.
23. **Jodko, D.; Obidowski, D.; Reorowicz, P; Jóźwik, K.** 2014. Simulations of the blood flow in the arteriovenous fistula for haemodialysisActa of Bioengineering and Biomechanics 16(1): 69-74.
https://doi.org/10.5277/abb14010.
24. **Keshavarz-Motamed, Z.; Kadem, L.** 2011. 3D pulsatile flow in a curved tube with coexisting model of aortic stenosis and coarctation of the aorta, Medical Engineering & Physics. 33: 315–324.
https://doi.org/10.1016/j.medengphy.2010. 10.017.

M. I. Arab, M. Bouzit, H. Ameur, Y. Kamla

NUMERICAL STUDY ON THORACIC AORTIC ANEURYSMS: THE ANEURYSM AGGRAVATION EFFECTS ON THE SECONDARY FLOW MOTION

S u m m a r y

It is well known that there is a strong correlation between artery wall diseases and the flow structure disturbance. Aneurysms are enlargements situated at different but specific parts of the vascular system; it is a silent disease that evolves in time. The Thoracic aortic aneurysm (TAA) remains relatively unstudied and therefore the present study aims is to clarify the effects of the (TAA) evolution and the geometrical variation on both hydrodynamic instabilities inside the aortic bulge especially the vortex ring phenomenon and the secondary motion (Dean and Lyne vortices) downstream the aneurysm. Two different cases of asymmetric enlargements in the ascending part of the aorta are studied for both Newtonian and the shear-thinning model to mimic the blood rheology inside the aneurysm bulge in order to investigate both parameters impact on the vortex ring behavior. Results showed that the blood rheology affects the propagation velocity while the aneurysm size influences the vortex ring rupture, the motion of the ring and its interaction shows similarities with the vortex ring interaction with an inclined wall phenomenon. Results also showed that vortex ring disturbs the boundary layer and therefore the secondary motion in the rest of the aorta.

Keywords: aneurysm, blood flow, Dean vortex, Lyne vortex, Vortex ring.

Received April 30, 2019
Accepted October 14, 2020